ELECTRONIC SUPPORTING INFORMATION

Estrone decorated poly-ion complex micelles for targeted melittin delivery to hormone responsive breast cancer cells

Radhika Raveendran, Fan Chen, Ben Kent, Martina H Stenzel

Materials

Unless otherwise specified, all chemicals were reagent grade and were used as received: Estrone, benzylamine, sodium triacetoxy borohydride (STAB-H), Palladium on carbon (Pd/C, 10 % wt loading), Poly (ethylene glycol) methyl ether methacrylate (OEGMEMA, M_n = 300 g mol^{-1}), *tert*-butyl methacrylate (^{t}BuMA, M_n = 80 g mol^{-1}) were purchased from Sigma-Aldrich and de-inhibited, by passing over a short column of basic alumina, prior to use. 2,2′-Azobis(isobutyronitrile) (AIBN, Fluka, 98%) was purified by recrystallization from methanol.

N-hydroxysuccinimide (NHS, 98%), N(3-(dimethylamino)propyl)-N'-ethylcarbodiimide hydrochloride (DCC,) trifluoroacetic acid, melittin [from honey bee venom ≥85% (HPLC)], and dibenzocyclooctyne-amine were purchased from Sigma-Aldrich. Diethyl ether (99%), toluene (>99.5%), dimethyl sulfoxide (DMSO, 98%) 1,2 dichloroethane, dichloromethane (DCM), sodium carbonate were purchased from Ajax Finechem. 4-cyano-4-[(phenylcarbonothioyl)thio]-pentanoic acid (CPADB) was synthesized according to a previous report (Roth, Collin et al. 2013). Tetrahydrofuran (THF), N, N-dimethylacetamide (DMAc, HPLC grade were purchased from Aldrich. Cyanine5 amine (Deuterated solvents mainly chloroform-d (CDCl3), dimethyl sulfoxide-d6 (DMSO-d6) and deuterated methanol (MeOD) were from Cambridge Isotope Laboratories. Cyanine 5 amine (Cy5) was purchased from Lumiprobe.

Analysis techniques

Nuclear Magnetic resonance

NMR spectroscopic measurements were performed on Bruker Avance III HD 400 MHz (^{1}H: 400.13 MHz)) instrument. NMR spectra were processed using the Bruker TOPSPIN 3.2 software.

LC/MS

LC/MS analysis was performed using a Phenomenex AerisXB-C18 column (3.6 µm, 2.1 x 100 mm) on Shimadzu LCMS 8030. The mobile phase consisted of milli-Q water with 0.05% ammonium hydroxide (Mobile Phase A), and HPLC grade methanol with 0.05% ammonium hydroxide (Mobile Phase B) at a flow rate of 0.2 mL/min, starting at 95% Mobile Phase A and 5% Mobile Phase B.

Size Exclusion Chromatography (SEC)

SEC was performed on a Shimadzu system equipped with four 300 × 7.8 mm linear phenogel columns (105, 104, 103, and 500 Å) and a 50 × 7.8 mm guard column. A flow rate of 1 mL min^{-1} was maintained using N, N′-dimethylacetamide (HPLC grade, 0.05% w/v BHT, 0.03% w/v LiBr) as eluent. Calibration of the system was performed with a series of narrow molar mass distribution poly (methyl methacrylate) with molar masses ranging from 0.58−1820 kg mol^{-1}.

Dynamic Light Scattering (DLS)

DLS experiments were conducted on a Malvern Zetasizer Nano ZS instrument equipped with a 4 mV He-Ne laser operating at $\lambda = 632$ nm and non-invasive backscatter detection at 173°. For a given sample, a total of three measurements were conducted with the number of runs, attenuator, and path length being automatically adjusted by the instrument, measurements were taken in triplicate and were carried out in a disposable cuvette at 25 °C.

Transmission Electron Microscopy (TEM)

TEM Analyses were performed on an FEI Tecnai G2 TEM operating at an accelerating voltage of 200 kV. Images were acquired using a BM Eagle 2K CCD Camera and an in-built low-dose software. 10 µl PIC micelle solution was pipetted onto a 200 mesh copper grid with formvar and carbon film support. The sample droplet was left for 2 minutes at room temperature, before blotted with filter paper. The grids were negatively stained with uranyl acetate for 2 minutes before blotting with filter paper and left to air-dry overnight prior to analysis.

Small-Angle X-ray scattering (SAXS)

SAXS measurements were performed on the SAXS/WAXS beamline at the Australian Synchrotron, ANSTO. SAXS patterns were recorded on a Pilatus 1M detector with an incident x-ray energy of 11.5 keV and a sample to detector distance of 2.4 m. The total q range covered was 0.005 – 0.5 $Å^{-1}$. Samples were loaded into a well plate, then circulated through a measurement capillary during measurement to avoid radiation damage effects. Multiple one second exposures were summed together, then the background PBS measurement subtracted to improve the signal to noise ratio. Measurements were normalized to incident x-ray flux then radially averaged to produce 1D SAXS curves.

UV−visible spectroscopy

Varian Cary 300 UV−visible spectrophotometer (UV−vis) was used to determine the concentration of DBCO in the wavelength range of 200 nm -600 nm.

Fluorescence microscopy

Fluorescence measurements were performed on a CARY Eclipse fluorescence spectrophotometer at room temperature. The fluorescence intensity of Cy5 labelled PIC micelles.was measured at 660 nm with excitation wavelength of 642 nm and the excitation slit was 5 nm.

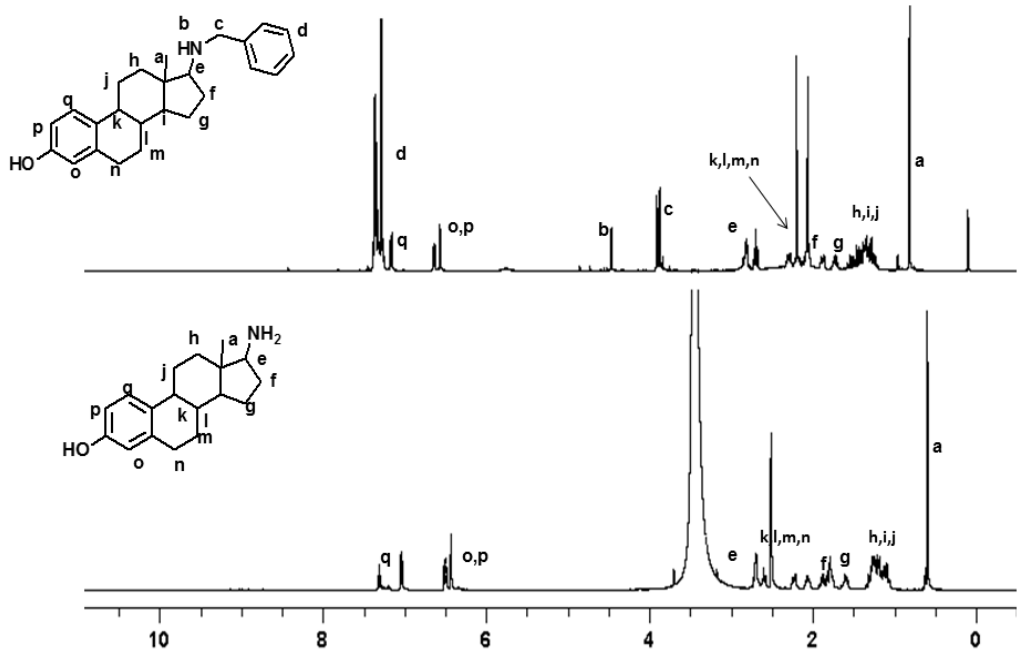

Figure S1. ^{1}H NMR spectra (A) 17 β-Benzylamino-1,3,5(10)-estratrien-3-ol
(B) 17 β-Amino-1,3,5(10)-estratrien-3-ol

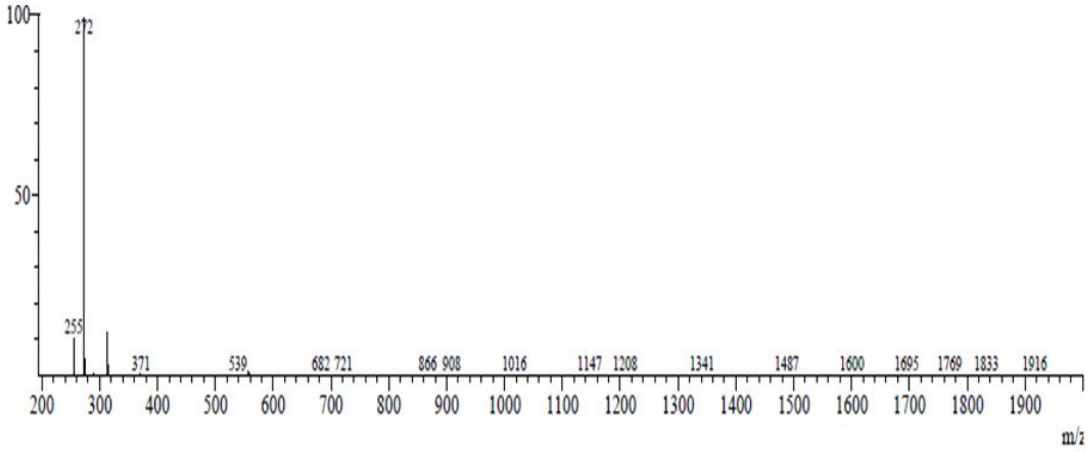

Figure S2. LC-MS of 17β-amino-1,3,5(10)-estratrien-3-ol

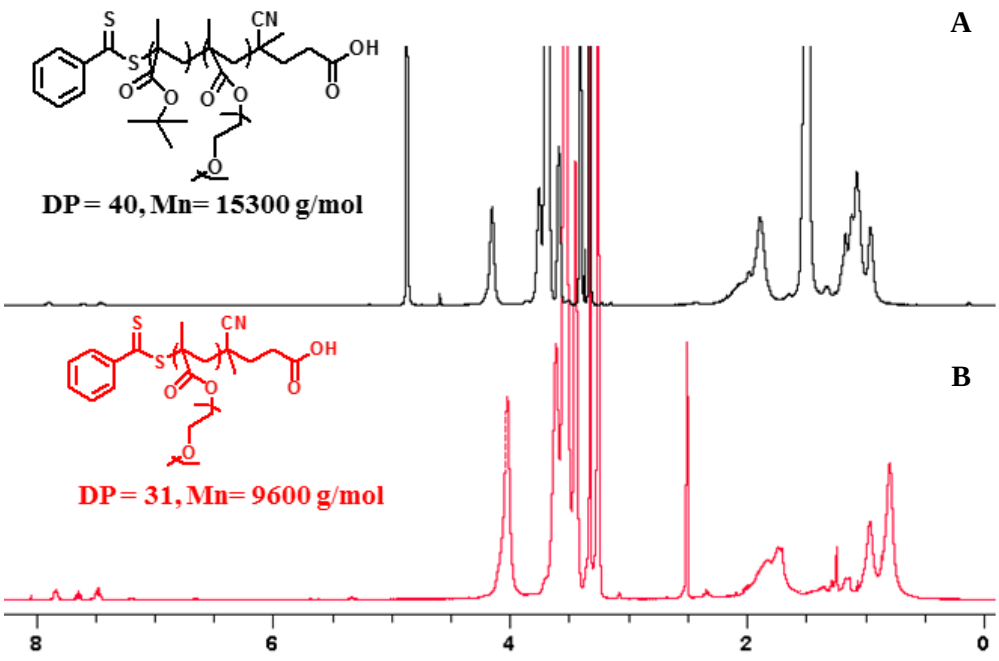

Figure S3. ^{1}H NMR spectra (A) POEGMEMA$_{31}$-P^{t}BuMA$_{40}$ (B) POEGMEMA$_{31}$

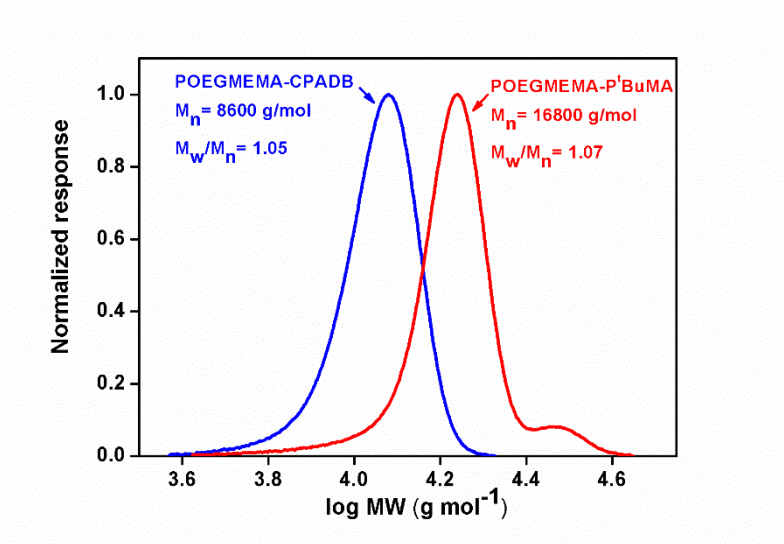

Figure S4. GPC chromatogram of POEGMEMA$_{31}$-P^{t}BuMA$_{40}$

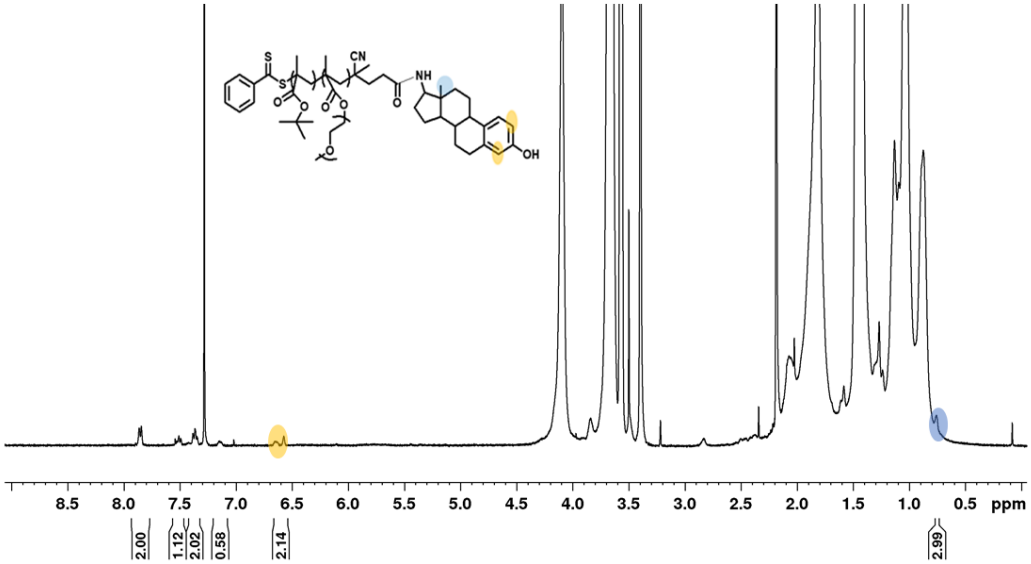

Figure S5. ^{1}H NMR spectrum of Estrone-POEGMEMA$_{31}$-PtBuMA$_{40}$

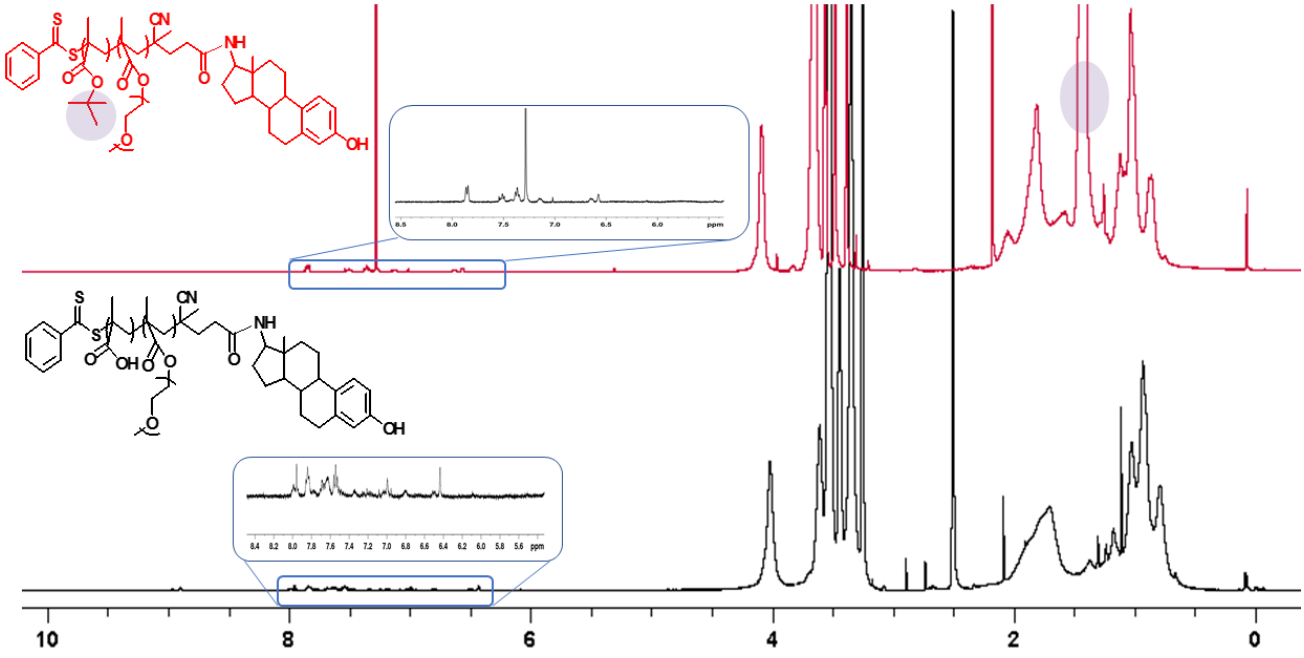

Figure S6. ^{1}H NMR spectra (A) Estrone- POEGMEMA$_{31}$-PtBuMA$_{40}$ (B) Estrone- POEGMEMA$_{31}$-PMAA$_{40}$. . Inset shows the magnified region between 6 ppm-8 pmm to indicate the presence of peaks corresponding to the protons of estrone

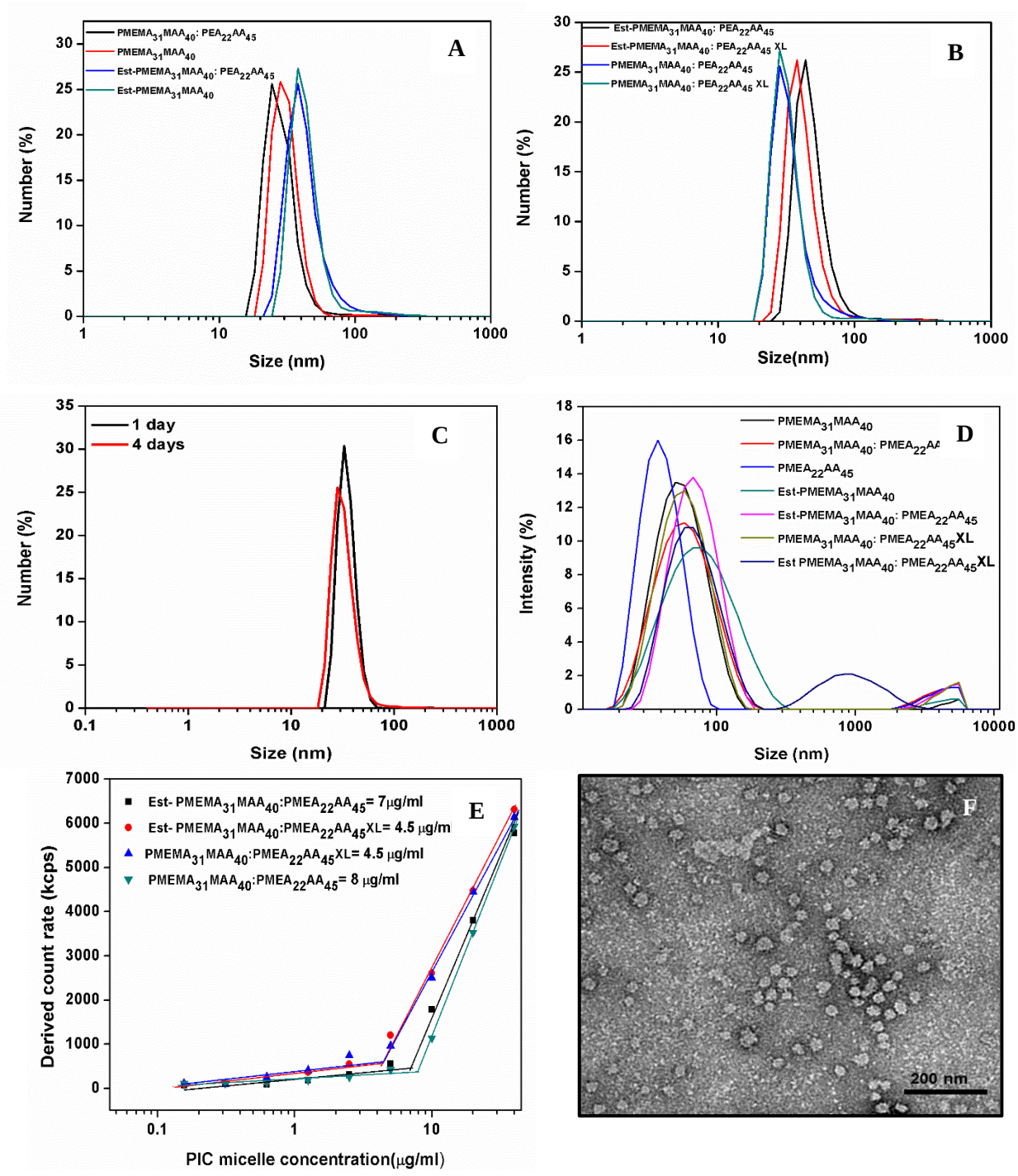

Figure S7. (A) Size of the mixed and unmixed micelles [number] (B)Size of crosslinked and un-crosslinked micelles [number](C) Size of crosslinked Estrone- $PMEMA_{31}$-$PMAA_{40}$:$POEGMEA_{22}$-PAA_{45} [number based](D) Intensity-size distribution of PIC micelles (E) Critical micelle concentration of the PIC micelles measured by DLS (F) Representative TEM image of Estrone-$PMEMA_{31}$-$PMAA_{40}$:$PMEA_{22}$-PAA_{45} [Scale bar = 200 nm]

Table S1. Fitting parameters of SAXS data

Parameters	P_1*	P_1 XL*	P_2*	P_2XL*
Volume Fraction	4.8 x 10^{-4}	5 x 10^{-4}	3.9 x 10^{-4}	4.8 x 10^{-4}
Mean radius (nm)	13	10.9	13.3	10.9
Polydispersity (sig/avg)	0.2	0.2	0.2	0.2
Interface thickness nm)	3.4	3.4	3.3	3.3
SLD sphere (A^{-2})	1.17 x10^{-5}	1.17 x 10^{-5}	1.17 x 10^{-5}	1.17 x 10^{-5}
SLD solvent(A^{-2})	9.45 x10^{-6}	9.45 x 10^{-6}	9.45 x 10^{-6}	9.45 x 10^{-6}
Lorentz scale	0.413	0.465	0.388	0.473
Lorentz length	135.78	135.78	135.78	135.78

* P_1 = $PMEMA_{31}$-$PMAA_{40}$ /$PMEA_{22}$-AA_{45}, P_1 XL* =$PMEMA_{31}$-$PMAA_{40}$ /$PMEA_{22}$-AA_{45} X L
P_2*=Est-$PMEMA_{31}$-$PMAA_{40}$ /$PMEA_{22}$-AA_{45}, P_2XL*=Est- $PMEMA_{31}$-$PMAA_{40}$ /$PMEA_{22}$-AA_{45} XL

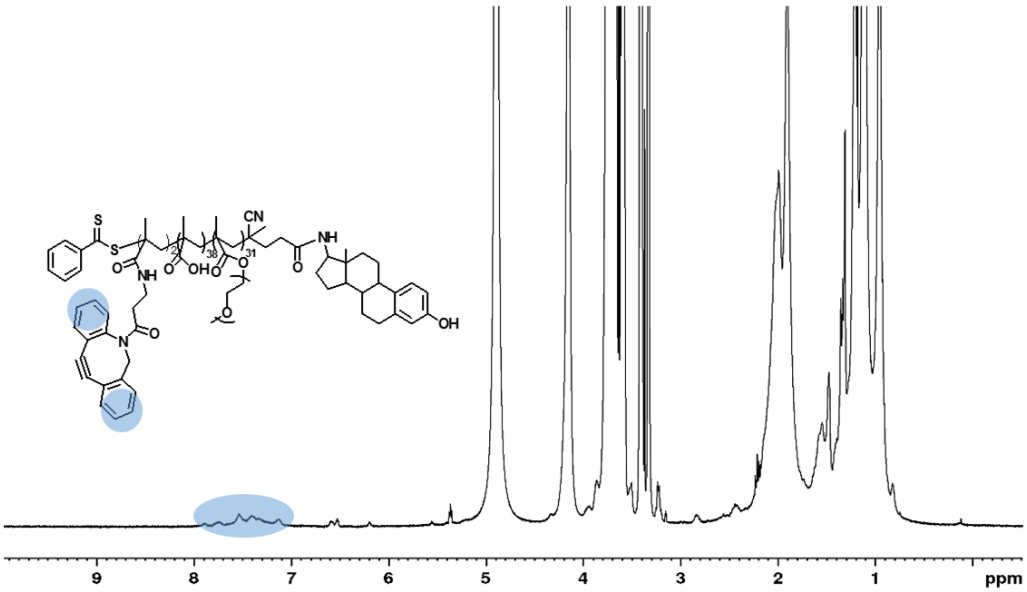

Figure S8. ^{1}H NMR spectra of DBCO conjugated Estrone- $POEGMEMA_{31}$-$PMAA_{40}$

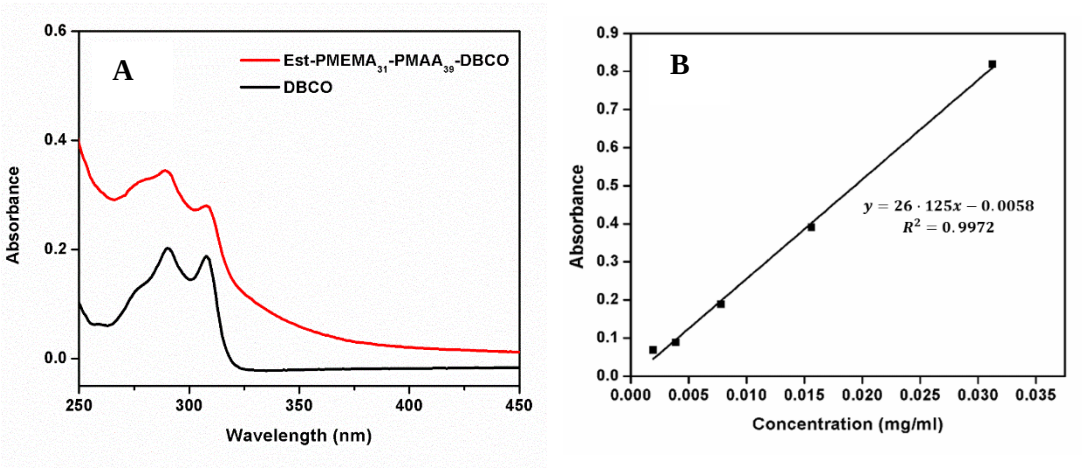

Figure S9. Determination of DBCO units attached to the polymer by UV-visible spectroscopy: (A) Absorption spectra(B) Calibration plot of Absorbance vs DBCO concentration to calculate the number of DBCO units

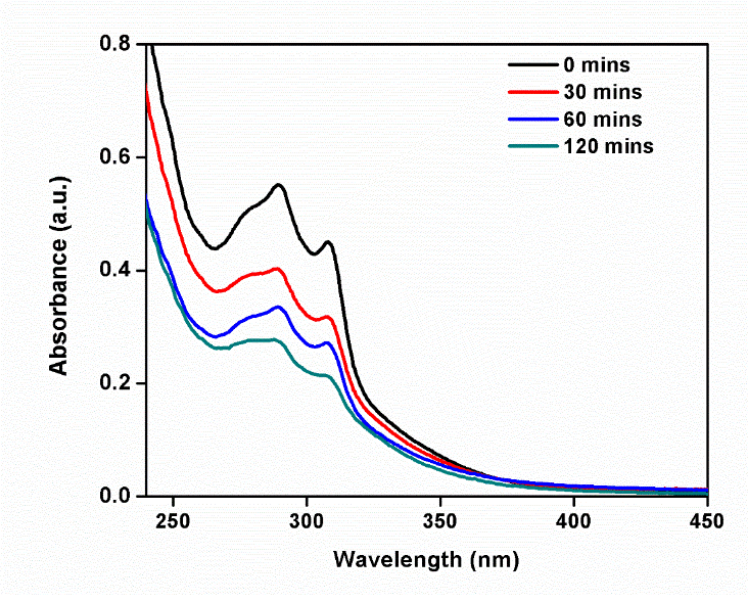

Figure S10. Reaction of DBCO bearing $POEGMEMA_{31}$-$PMAA_{40}$ and azide cross-linker monitored using UV-Vis spectroscopy

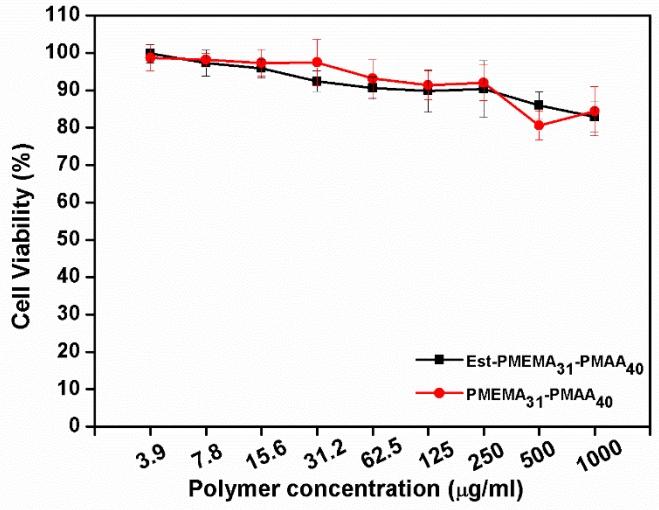

Figure S11. Cytotoxicity study on the synthesized polymers in MCF-7 cells after 48 h incubation.

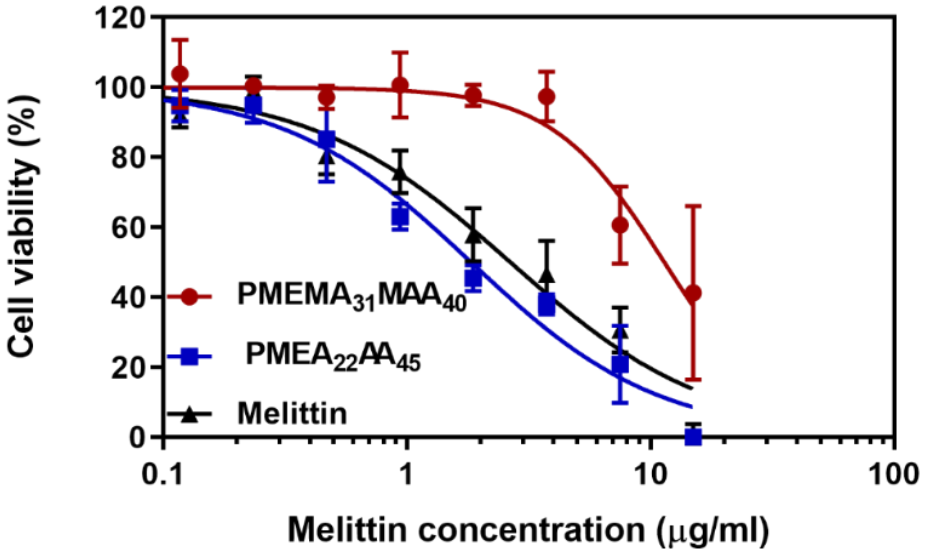

Figure S12. Cytotoxicity study on melittin complexed PIC micelles in MCF-7 cells after 72 h incubation

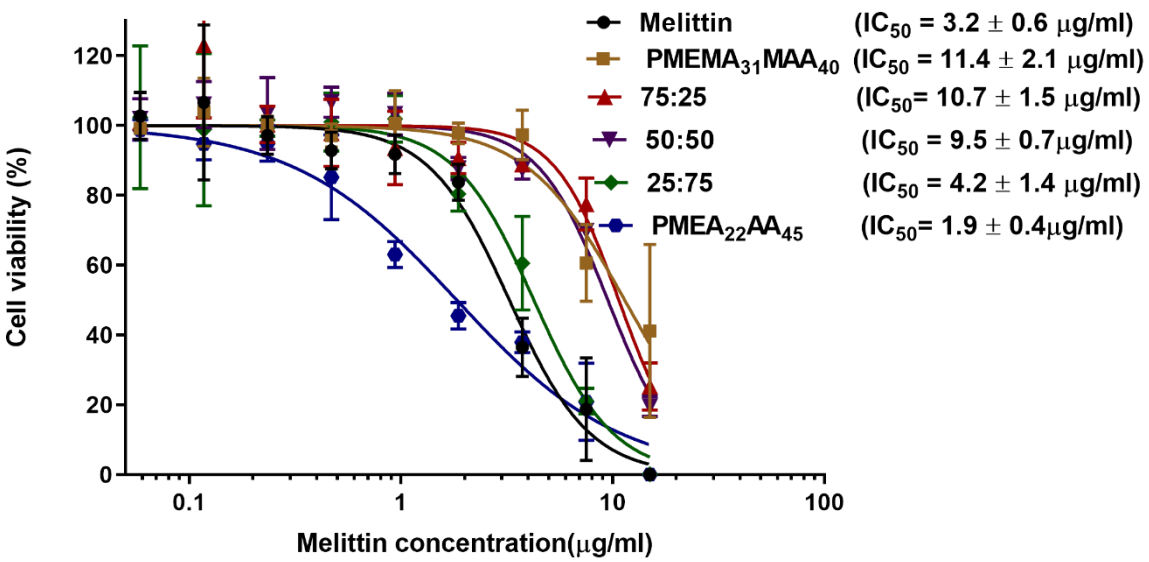

Figure S13. Cytotoxicity study on melittin complexed mixed PIC micelles of various ratios in MCF-7 cells after 72 h incubation

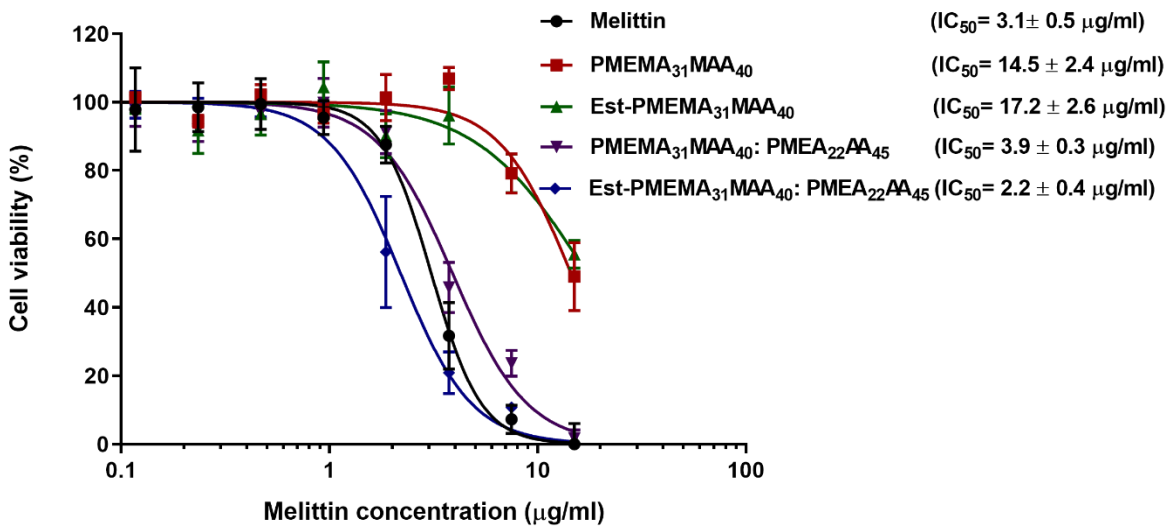

Figure S14. (A**)** Cytotoxicity study on melittin complexed mixed PIC micelles in MCF-7 cells after 72 h incubation. The ratio of $PMEMA_{31}$-$PMAA_{40}$ /$PMEA_{22}$-AA_{45} in the mixed micelles was 25:75

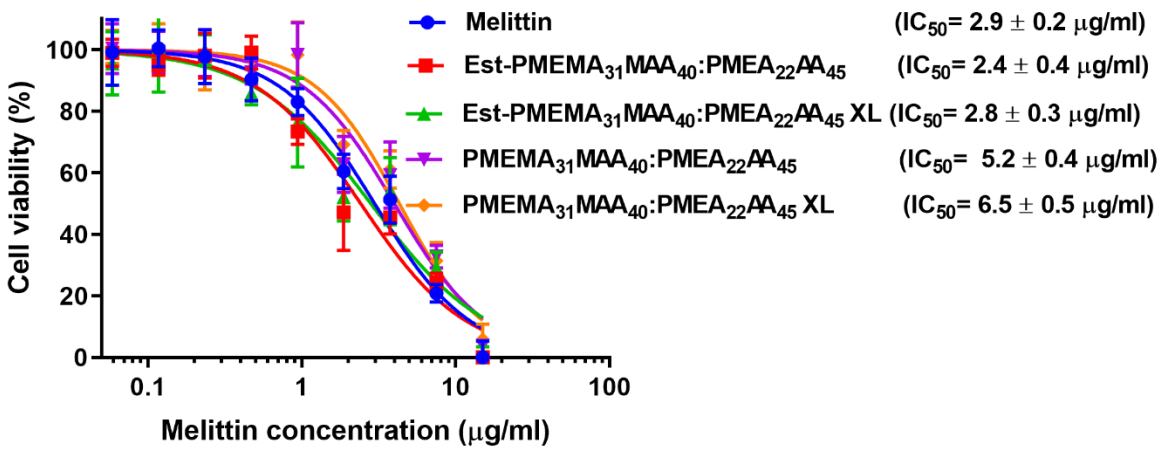

Figure S15. Cytotoxicity study on melittin complexed cross-linked mixed PIC micelles in MCF-7 cells after 72 h incubation. The ratio of $PMEMA_{31}$-$PMAA_{40}$ /$PMEA_{22}$-AA_{45} in the mixed micelles was 25:75

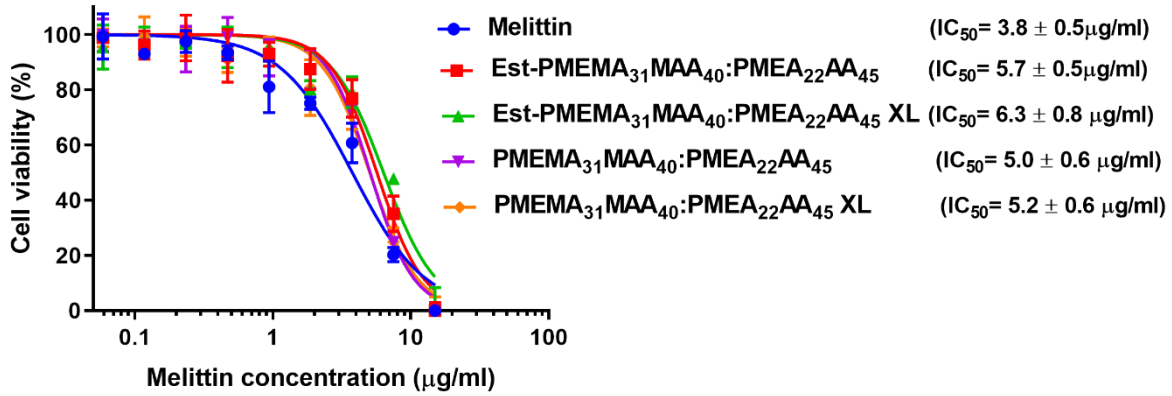

Figure S16. Cytotoxicity study on melittin complexed PIC micelles in MDA-MB-231cells after 72 h incubation. The ratio of $PMEMA_{31}$-$PMAA_{40}$ /$PMEA_{22}$-AA_{45} in the mixed micelles was 25:75

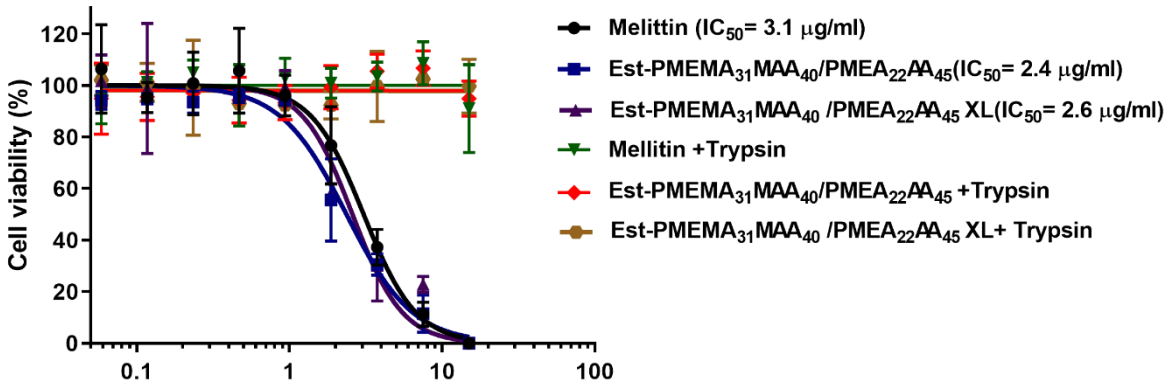

Figure S17. Cytotoxicity study on trypsin treated melittin complexed PIC micelles in MCF-7 cells after 72 h incubation. The starting concentration of melittin was 15 μg/ml. The ratio of $PMEMA_{31}$-$PMAA_{40}$ /$PMEA_{22}$-AA_{45} in the mixed micelles was 25:75

Table S2. Mean Fluorescence Intensity of MCF-7 cells with internalized PIC Micelles measured by flow cytometry.

Sample	Fluorescence intensity [a] (a.u)	Normalization factor	Normalized mean fluorescence intensity[b]
$PMEMA_{31}$-$PMAA_{40}$:PEA_{22}-PAA_{45}	20.5	0.67	854 ± 132
$PMEMA_{31}$-$PMAA_{40}$:PEA_{22}-PAA_{45} XL	29.9	0.97	1271±52
Est-$PMEMA_{31}$-$PMAA_{40}$:PEA_{22}-PAA_{45}	30.8	1	6164±42
Est-$PMEMA_{31}$-$PMAA_{40}$:PEA_{22}-PAA_{45}XL	29.8	0.97	4217±147
Control	-	-	73±1

[a] The fluorescence intensity was measured at 660 nm with excitation wavelength of 642 nm by fluorescence spectrometer after 4 times dilution .[b] The normalized mean fluorescence intensity values were determined by normalizing the mean fluorescence intensity obtained from flow cytometry experiment with the factors shown in column after subtraction of the autofluorescence from the control sample.

Table S3. Mean Fluorescence Intensity of MDA-MB-231 cells with internalized PIC Micelles measured by flow cytometry.

Sample	Fluorescence intensity [a] (a.u)	Normalization factor	Normalized mean fluorescence intensity[b]
$PMEMA_{31}$-$PMAA_{40}$:PEA_{22}-PAA_{45}	19.2	0.65	620 ± 15
$PMEMA_{31}$-$PMAA_{40}$:PEA_{22}-PAA_{45} XL	18.6	0.63	630±31
Est-$PMEMA_{31}$-$PMAA_{40}$:PEA_{22}-PAA_{45}	29.5	1	758±11
Est-$PMEMA_{31}$-$PMAA_{40}$:PEA_{22}-PAA_{45}XL	18.1	0.61	658±16
Control	-	-	68±1

[a] The fluorescence intensity was measured at 660 nm with excitation wavelength of 642 nm by fluorescence spectrometer after 4 times dilution.[b] The normalized mean fluorescence intensity values were determined by normalizing the mean fluorescence intensity obtained from flow cytometry experiment with the factors shown in column after subtraction of the autofluorescence from the control sample.

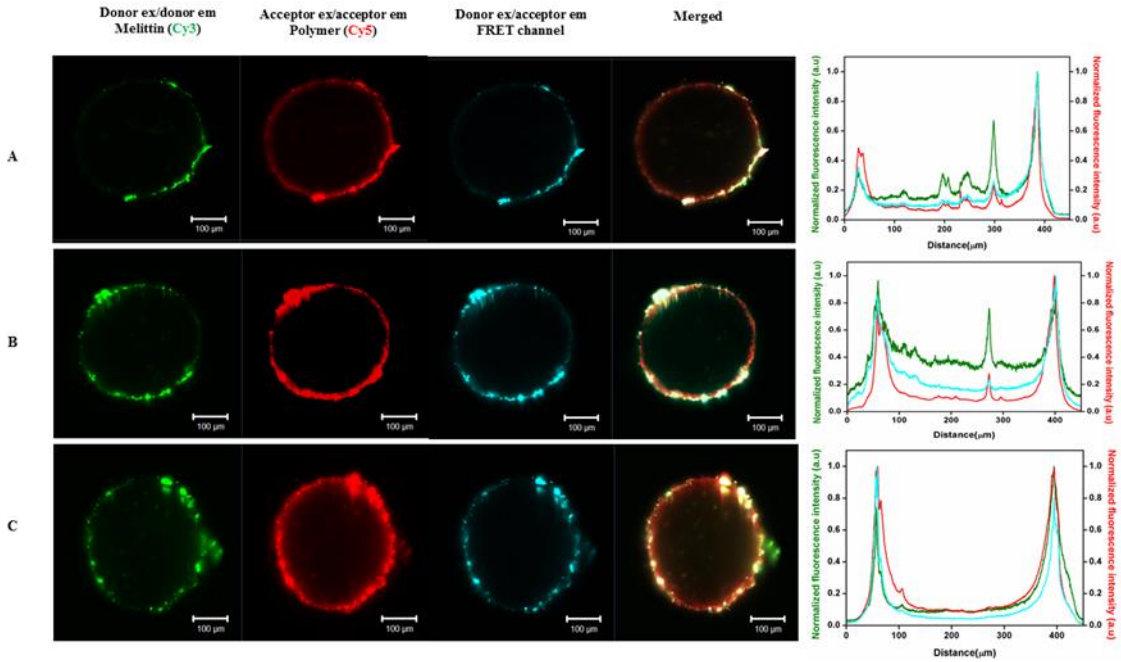

Figure 18 (Left) Light sheet microscopy images depicting the penetration ability of PIC micelles (A) $POEGMEA_{22}$-PAA_{45} /$POEGMEMA_{31}$-$PMAA_{40}$ (B) Est-$POEGMEA_{22}$-PAA_{45} /$POEGMEMA_{31}$-$PMAA_{40}$ and (C) Est-$POEGMEA_{22}$-PAA_{45} /$POEGMEMA_{31}$-$PMAA_{40}$ XL after an incubation time of 2 h. (Right) Corresponding Fluorescence intensity profiles of the penetrated PIC micelles

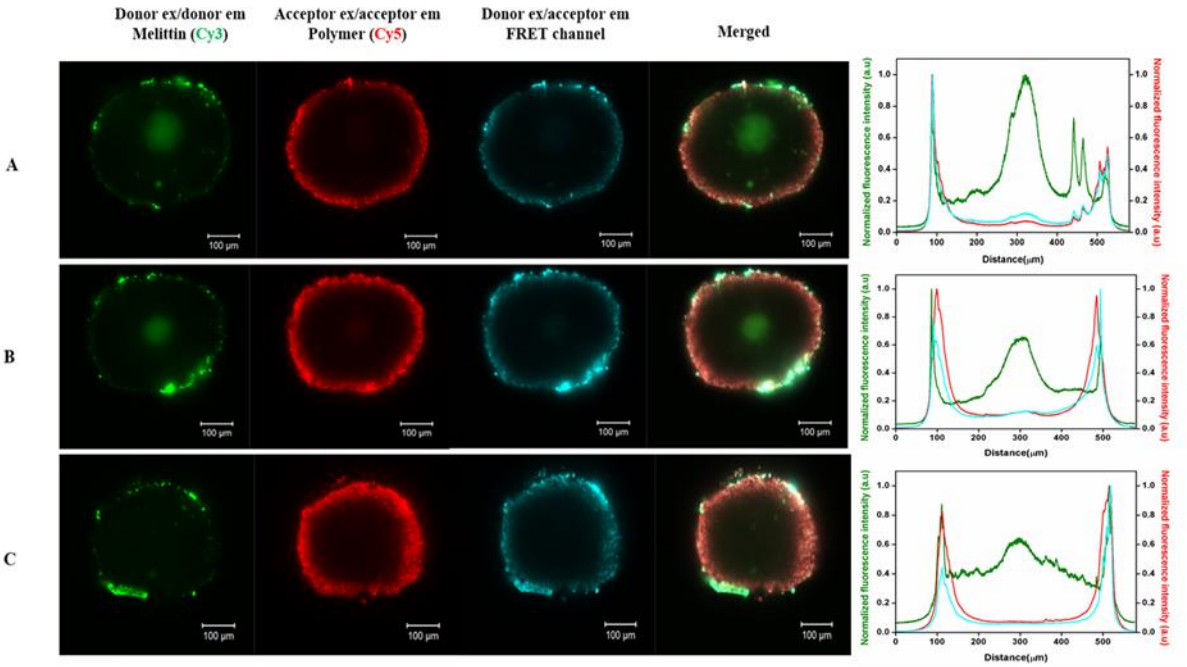

Figure 19 (Left) Light sheet microscopy images depicting the penetration ability of PIC micelles (A) POEGMEA$_{22}$-PAA$_{45}$ /POEGMEMA$_{31}$-PMAA$_{40}$ (B) Est-POEGMEA$_{22}$-PAA$_{45}$ /POEGMEMA$_{31}$-PMAA$_{40}$ and (C) Est-POEGMEA$_{22}$-PAA$_{45}$ /POEGMEMA$_{31}$-PMAA$_{40}$ XL after an incubation time of 6 h. (Right) Corresponding Fluorescence intensity profiles of the penetrated PIC micelles

References

Roth, P. J., et al. (2013). "Advancing the boundary of insolubility of non-linear PEG-analogues in alcohols: UCST transitions in ethanol–water mixtures." Soft Matter **9**(6): 1825-1834.